



Ab initio associative ionization calculations for Earth atmospheric entry

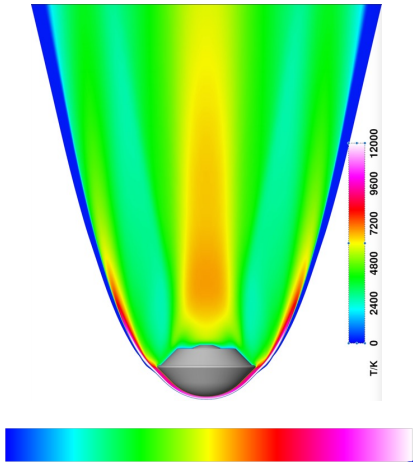
E Papajak
AMA Inc at Entry Systems and Technology Division, NASA Ames
D Schwenke
Advanced Supercomputing Division, NASA Ames

MURI kickoff meeting
Friday, December 2, 2022

Earth entry radiation

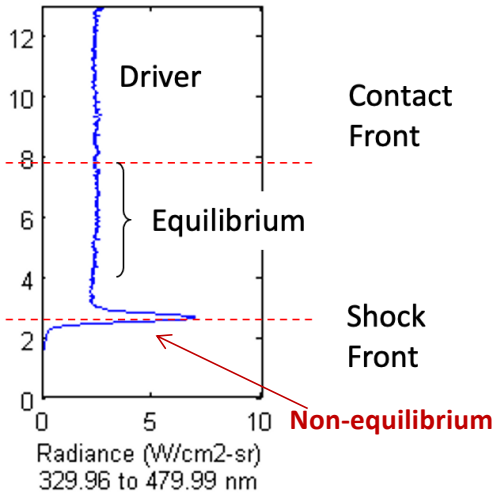
Hypersonic entry of a space vehicle into a planetary atmosphere

Hayabusa Earth entry



12.2 km/s entry[1]

EAST shock tube



Microseconds behind the shock!

	Earth entry conditions:	**DoD hypersonics MURI conditions of interest:**
Altitude:	~ 50 km	~ 30 km
Entry speed:	~ 10-12 km/s	~ 5-8 km/s
Temperature:	>> 10,000 K	~ 5-10,000 K

Generally longer durations

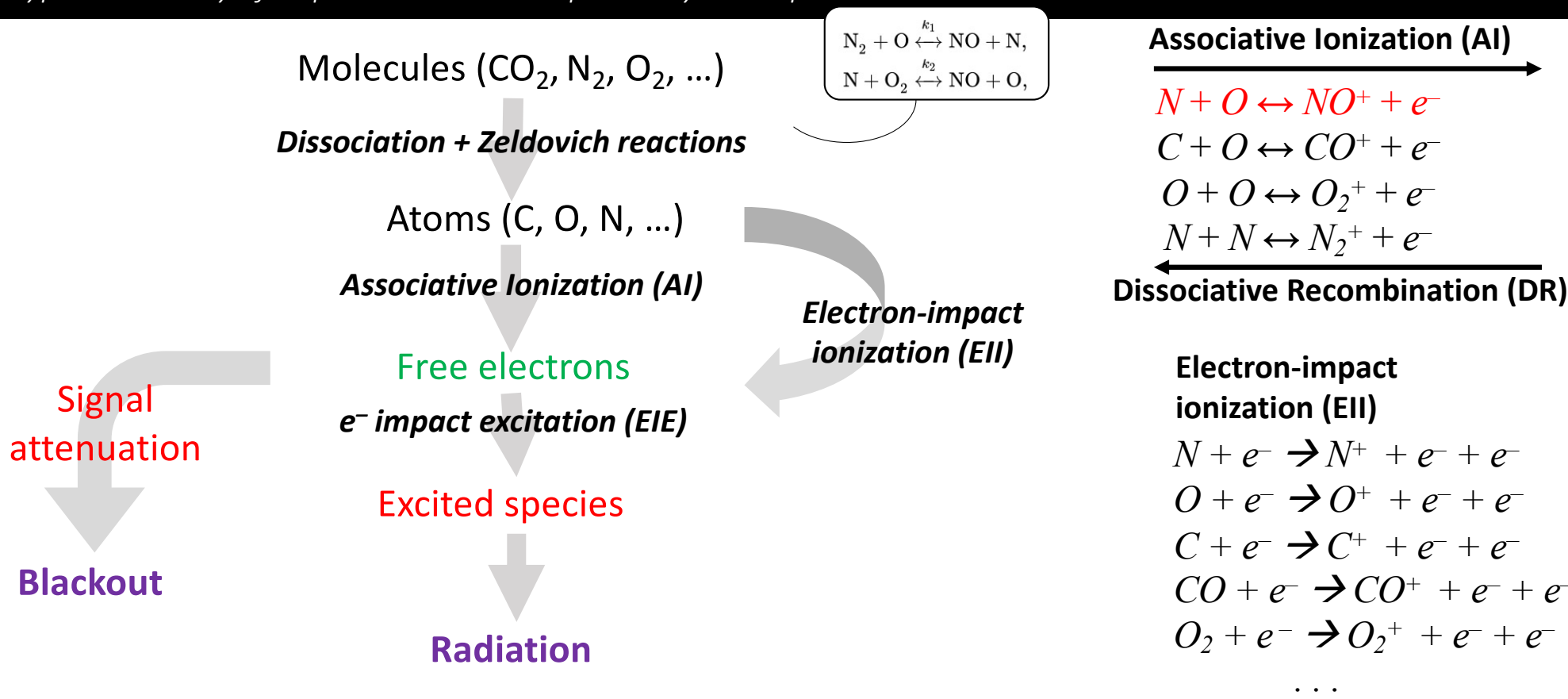
Challenges:

- hypersonic entry chemistry is fast (m-second time scale)
- significant portion of radiation comes from non-equilibrated excited species immediately behind the shock

[1]Figure credit: Dinesh Prabhu
[2]Figure credit: Brett Cruden

Earth entry radiation

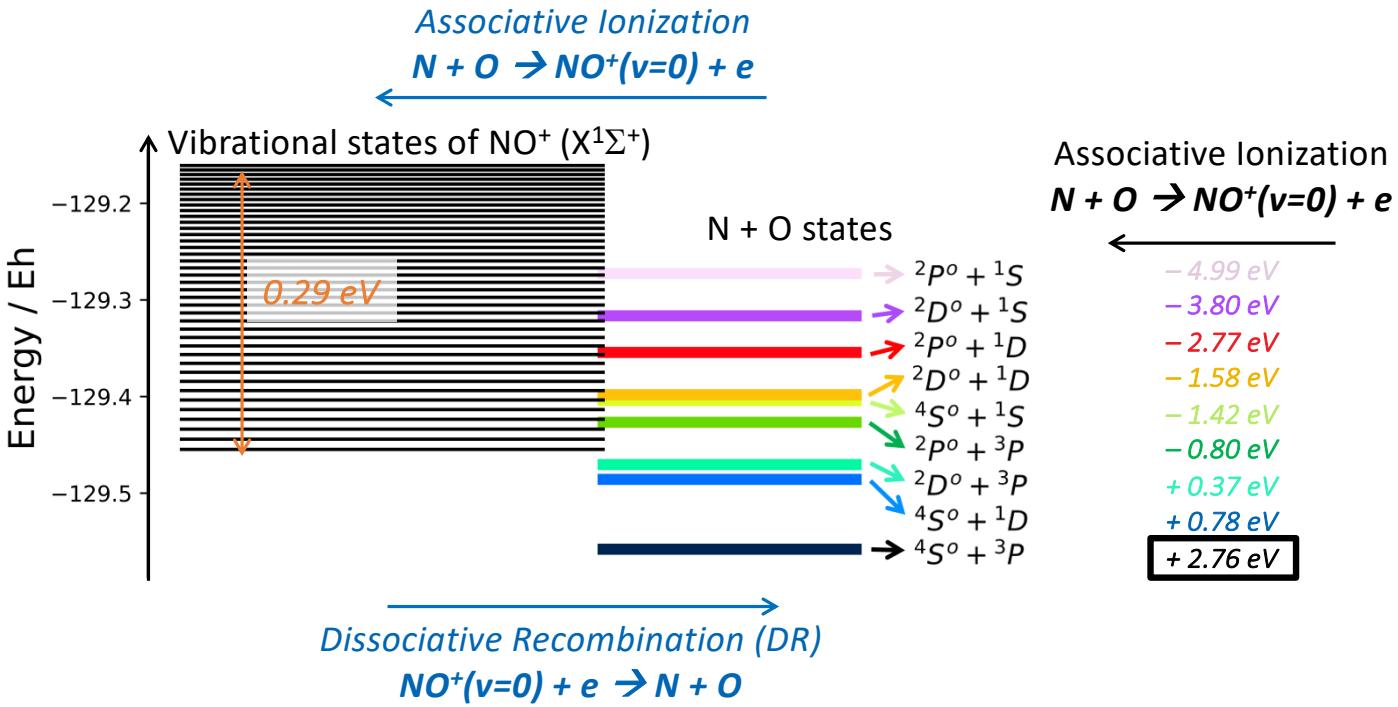
Hypersonic entry of a space vehicle into a planetary atmosphere



- N+O is the dominant mechanism of ionization initiation
- Ionization results in **radiative heat** and **communication attenuation**

AI reaction dynamics

Reaction energy and previous works



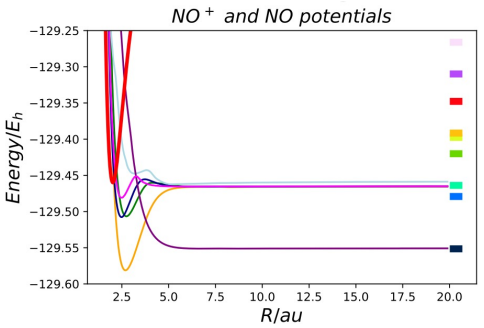
Literature: Experimental data

- mostly thermal conditions with contributions from different electronic states
- NO^++e forming metastable atoms is important in ionosphere
- Lin&Teare 1963 showed importance of N($^2D^o$)
- Ringer&Gentry 1979 merged beam experiment focuses on $^2D^o$+^3P
- N+O based on Dunn&Lordi DR (1969-1970) is used in flow field calculations

- AI for the lowest states of atoms is endoergic and becomes exoergic for higher metastable states
- Measurement by Lin&Teare and Ringer&Gentry point to $^2D^o$+^3P as a significant reactive channel

Potential curves for NO+ and NO

Electronic structure calculation credit: David Schwenke



- Electronic states NO+ ($X^1\Sigma^+$) and NO ($B^2\Pi$, $L^2\Pi$, $3^2\Pi$, $B'^2\Delta$, $A'^2\Sigma^+$, $I^2\Sigma^+$)

- Complete Active Space Self-Consistent Field internally contracted Multi-Reference Configuration Interaction method (CASSCF-icMRCI)

- A modified version of the MOLPRO quantum chemistry computer code is used to carry out the electronic structure calculation.
- The modifications of note for these calculations were the ability to converge to a particular Lambda^2 state: *e.g.* Sigma$^+$ and the Delta component falling in the A_1 symmetry block were computed in separate icMRCI calculations.

- To account for the Rydberg orbitals and O^- character in the wavefunctions, the basis set is augmented by the original diffuse functions from Dunning's "aug-" diffuse function sets. The basis on N is further augmented by single *spdf* functions and the basis on O is further augmented by two sets of *spdf* functions, with the exponential parameters determined an even tempered extension of the existing basis.

- Careful generation of Rydberg states

AI reaction dynamics

Wave packet calculations

Time-dependent Schrodinger eqn.

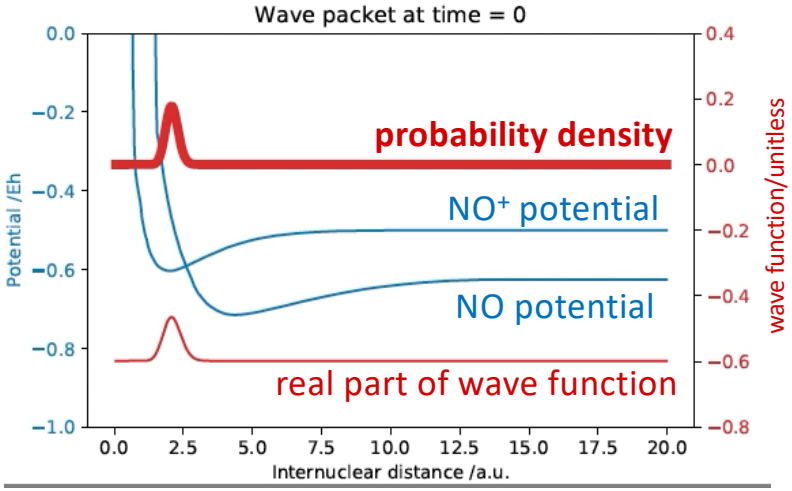
$$i\frac{\partial}{\partial t}\Psi(\boldsymbol{r},t) = H(\boldsymbol{r},t)\Psi(\boldsymbol{r},t)$$

Initial wave packet

$$\Psi(R,t=0) = V_E(\mathrm{R})\chi_{vi}(R)$$

$V_E(\mathrm{R})$: electronic coupling from R-matrix

$\chi_{vi}(R)$: vibrational states of the cation



Nuclear motion dynamics involves solving time-dependent Schrodinger equation for a wave packet on a complex potential

$$H = -\frac{1}{2\mu}\frac{\partial^2}{\partial R^2} + E_{res}(R) - i\frac{\Gamma(R)}{2}$$

$\Gamma(R)$: autoionization width

$$\Gamma(R) = 2\pi|V_E(R)|^2$$

$V_E(R)$: electronic coupling

Schneider & Tennyson R-matrix

2000 *J. Phys. B: At. Mol. Opt. Phys.* **33** 4849

Resulting wave function evolution in time represents dissociating atoms in time

AI reaction dynamics

Wave packet calculations

Cross sections as a function of collision energy

$$\sigma(E) = \frac{2\pi^3}{E}|T(E)|^2$$

$$T(E) = -\frac{i}{\hbar}\int_0^\infty e^{\frac{iEt}{\hbar}}\left\langle \phi_{v_f}\middle|\Psi_{v_i}(t,R)\right\rangle dt$$

plane waves (represent dissociating N+O atoms with varying amounts of kinetic energy)

wavefunction (as calculated at every point in time)

AI cross sections:

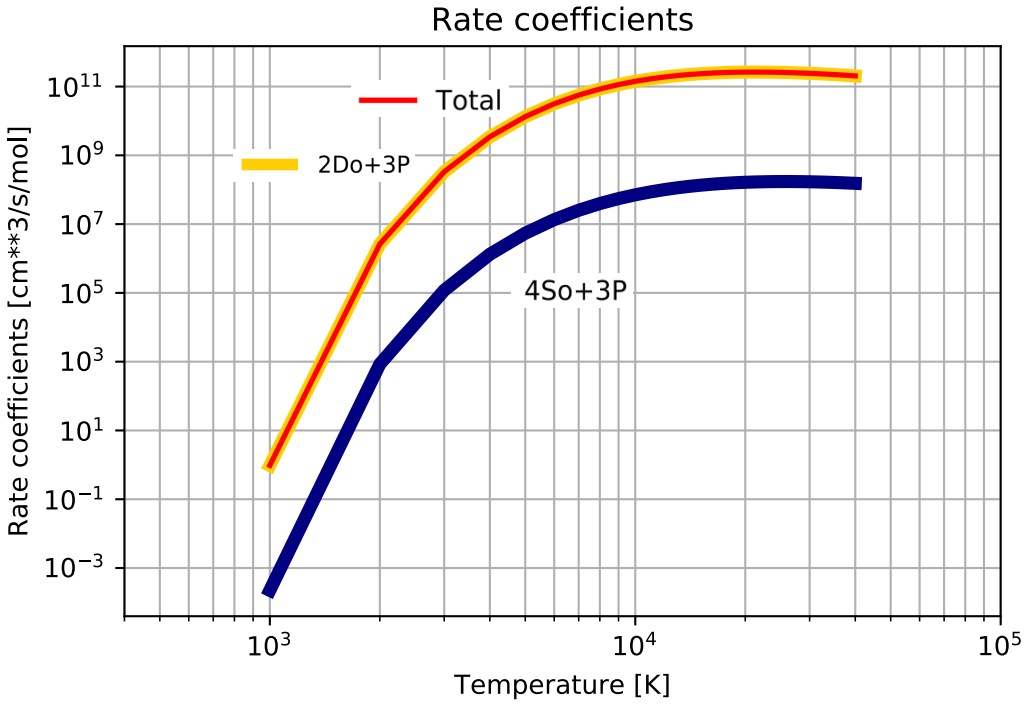
$$\sigma_{AI}(E_{N+O}) = \frac{\mu_{NO^+ + e^-}\, E_{NO^+ + e^-}\, g_{NO^+} g_{e^-}}{\mu_{N+O}\, E_{N+O}\, g_N g_O}\sigma_{DR}(E_{NO^+ + e^-})$$

Rate coefficients:

$$k(v,T) = \left(\frac{1}{\pi\mu}\right)^{1/2}\left(\frac{2}{k_B T}\right)^{3/2}\int_0^\infty \sigma(E)\, E e^{-E/k_B T} dE$$

Thermal rate coefficients:

$$k(T) = \sum_{v=0}^{N} e^{-\frac{E_v}{k_B T}} k(v,T)$$

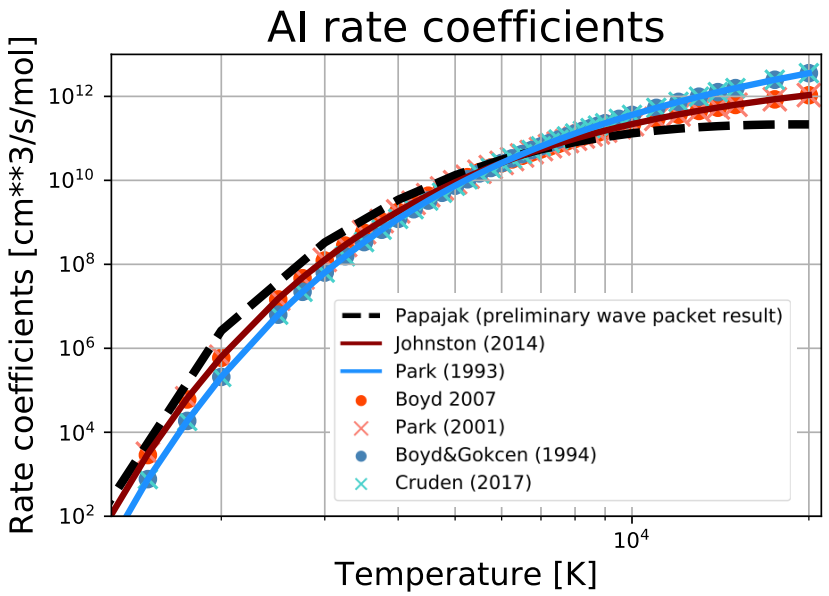


B $^2\Pi$ dominates at low-T leading to $^2D^o + ^3P$

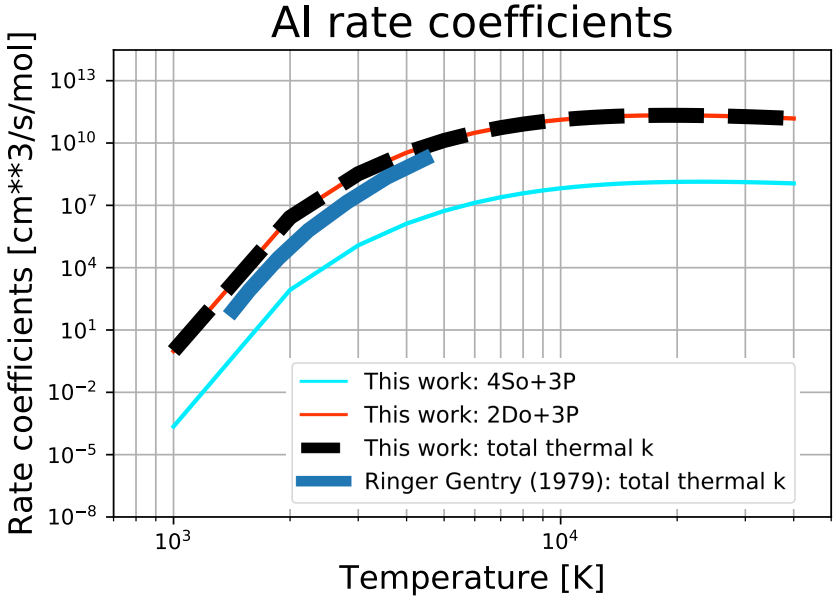
AI reaction dynamics

Wave packet calculations

Comparison with AI rate coefficients derived from Dunn & Lordi DR experiment used in re-entry chemistry modeling



Comparison with Ringer & Gentry AI experiment



- Our total AI rate coefficient is higher than that of Ringer & Gentry's, but lower than Dunn & Lordi-derived ones
- Slope matches Ringer&Gentry, but is lower than that of Dunn&Lordi.

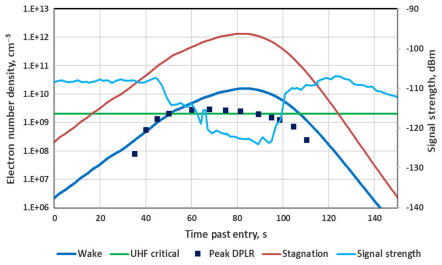
Communication blackout prediction

Attenuation calculations for Mars 2020

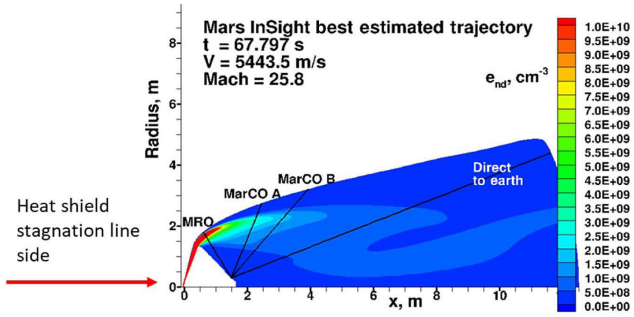
- Reliable communication provides more options
  - Continuous telemetry and diagnostics in event of failure
  - Assistance from ground
  - In case of a mishap, more data → safety of future missions
  - Tracking
- Must understand the cause of blackout to mitigate it

Apollo 13: re-entry blackout lasted ~1 min 30 seconds longer than expected

Mars InSight observed a blackout period of approximately 45 seconds [1]



Attenuation still present when density goes subcritical



Flow ionizes → dense plasma forms. Plasma has fundamental frequency…

$$\omega_p = \sqrt{\frac{n_e e^2}{\epsilon_0 m_e}} \qquad n_e \equiv \text{Electron number density}$$

When plasma frequency exceeds radio frequency, attenuation occurs

$$\frac{\omega_p}{2\pi} = f_p > f_{\text{UHF}} \approx 400 \text{ MHz}$$

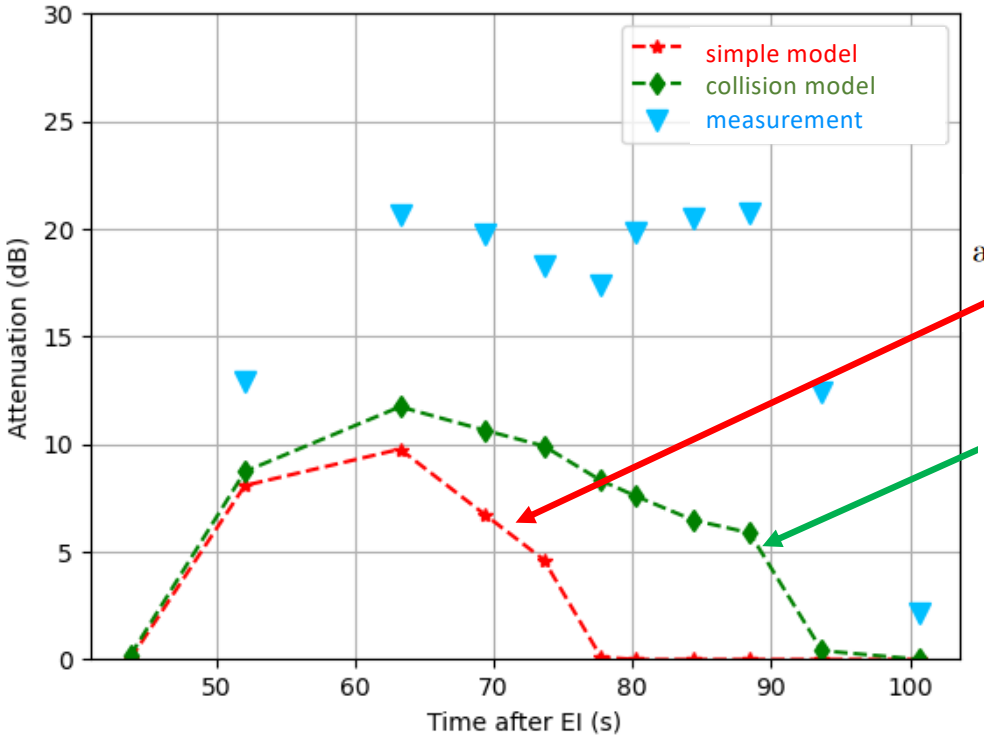
Critical electron density at which $f_p = f_{radio} \Rightarrow n_{e,crit} = 2 \times 10^{15} \text{ m}^{-3}$

$$\text{Predicted attenuation (dB)} = 20 \log_{10} \left\{ \exp \left[\frac{2\pi f}{c} \int_0^s \left(\frac{n_e e^2}{4\pi^2 \epsilon_0 m_e f^2} - 1 \right)^{1/2} ds \right] \right\}$$

Previous work at JPL showed importance of N+O

Communication blackout prediction

Attenuation calculations for Mars 2020



Comparison of attenuation with vs without electron collisions:

$$\text{attenuation (dB)} = 20\log_{10}\left\{\exp\left[\frac{2\pi f}{c}\int_0^s\left(\frac{n_e e^2}{4\pi^2\epsilon_0 m_e f^2}-1\right)^{1/2}ds\right]\right\}$$

$$A_{dB} = 20\log_{10}(e)\left(\frac{\omega}{c}\right)\int_0^s\sqrt{\left((K_r^2+K_i^2)^{1/2}-K_r\right)/2}\;ds$$

Mehra (2015) provides attenuation model that incorporates the effect of electron-nonelectron collisions

Longer “tail” in the improved blackout model better matches measured attenuation!

Conclusions



- Revisiting this reaction is important to improve upon outdated non-state specific models

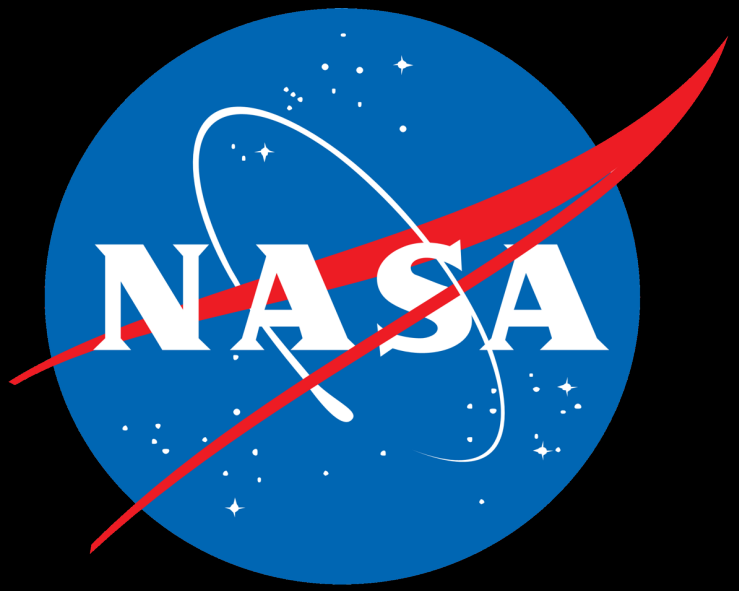
- New ab initio potential energy curves

- New cross sections and rates
  - –new rates
  - –state-specific rate information – improved models beyond T/Tv
  - –$^2D^o+^3P$ through B $^2\Pi$ is the main reaction mechanism

- Our total AI rate coefficient is higher than that of Ringer&Gentry's, but matches the orders of magnitude of Dunn&Lordi–derived ones.

- Temperature dependence of the AI ab-initio rate coefficient is less steep than that of the chemistry models now in use for re-entry modeling.

National Aeronautics and Space Administration



Ames Research Center
Entry Systems and Technology Division